Astrophysical factors of ^{12}C+^{12}C fusion extracted using the Trojan horse method

A. M. Mukhamedzhanov, D. Y. Pang, and A. S. Kadyrov

Phys. Rev. C **99**, 064618 — Published 27 June 2019

DOI: 10.1103/PhysRevC.99.064618

Astrophysical factors of $^{12}C + ^{12}C$ fusion extracted using Trojan Horse method

A. M. Mukhamedzhanov,[1,*] D. Y. Pang,[2,3,†] and A.S. Kadyrov[4,‡]

[1] *Cyclotron Institute, Texas A&M University, College Station, TX 77843, USA*
[2] *School of Physics and Nuclear Energy Engineering, Beihang University, Beijing, 100191,People's Republic of China*
[3] *Beijing Key Laboratory of Advanced Nuclear Materials and Physics, Beihang University, Beijing 100191, China*
[4] *Curtin Institute for Computation and Department of Physics and Astronomy, Curtin University, GPO Box U1987, Perth, WA 6845, Australia*

Carbon-carbon burning plays an important role in many stellar environments. Recently, Tumino *et al.* [Nature **557**, 687 (2018)] reported a sharp rise of the astrophysical S factor for carbon-carbon fusion determined using the indirect Trojan Horse method. We demonstrate that the rise at low energies seen in the aforementioned work is an artefact of using an invalid plane-wave approximation that neglects the Coulomb interactions. Our analysis shows that such a rise disappears if the Coulomb (or Coulomb-nuclear) interactions in the initial and final states are included.

PACS numbers: 25.60.Pj, 25.40.Hs, 26.30.-k,24.10.-i

I. INTRODUCTION

Recently, the indirect Trojan Horse method (THM) was applied to measure the astrophysical S^* factor of $^{12}C + ^{12}C$ fusion [1]. The method is based on using a surrogate Trojan Horse (TH) reaction $a(sx) + A \to s + F(xA) \to s + b + B$ to determine the astrophysical $S^*(E)$ factor of the binary resonant subreaction $x + A \to F \to b + B$. In the case under consideration $a = {}^{14}N$, $A = {}^{12}C$, $x = {}^{12}C$, $s = d$, and $F = {}^{24}Mg^*$. Four different channels in the final state were populated in the THM experiment: $p_0 + {}^{23}Na$, $p_1 + {}^{23}Na$ (0.44 MeV), $\alpha_0 + {}^{20}Ne$, and $\alpha_1 + {}^{20}Ne$ (1.63 MeV) [1]. To analyze the measured data Tumino *et al.* [1] used a simple plane-wave approximation (PWA) developed by one of us (A.M.M.). This approximation neglects the Coulomb interactions between the fragments. In Refs. [2, 3], a generalized R-matrix approach was developed within the surface integral formalism [4]. The approach uses distorted waves in both initial and final states (see Eq. (117) of Ref. [2]). The PWA follows from this more general approach when the distorted waves are replaced with the plane waves. The PWA was successfully applied for analyses of many THM reactions in which the spectator is a neutron. It was also applied to reactions at energies above the Coulomb barrier in the initial and final states, and when the interacting nuclei have small charges [5, 6]. In the PWA it is assumed that the angular distribution of the spectator is forward-peaked in the center-of-mass system (quasi-free kinematics) and that the bound-state wave function of the spectator can be factorized out (see Eq. (117) of Ref. [2] and Eq. (2) of Ref. [1]). Usage of the PWA can be justified only if the PWA and the distorted-wave-Born approximation (DWBA) give similar energy dependence for the differential cross section (DCS) of the transfer reaction. This is because in the THM only the energy dependence of the astrophysical factor is measured while its absolute value is determined by normalizing the THM data to available direct data at higher energies.

Tumino *et al.* [1] reported that the astrophysical $S^*(E)$ factors extracted from the THM experiment demonstrate a steep rise when the resonance energy E decreases. This rise would have profound implications on different astrophysical scenarios as the carbon-carbon fusion rate calculated from the astrophysical S^* factors deduced in Ref. [1] significantly exceeds all previous estimations of the reaction rate obtained by extrapolating the direct data to the low-energy region. For example, the reaction rate calculated in Ref. [1] at temperature $T \sim 2 \times 10^8$ K exceeds the adopted value [7, 8] by a factor of 500.

The authors of Ref. [1] were rightly concerned about the Coulomb barrier in the initial state. That is why in the experiment the initial energy was above the Coulomb barrier. However, given the energy of the emitted particles, neglecting the Coulomb effects in the final channel is unjustified. The purpose of this paper is to present a detailed analysis of the TH resonant reactions based on the distorted-wave formalism. We take into account the distortions in the initial, intermediate and final states. The THM triple DCS is expressed in terms of the THM amplitude obtained in Appendix A.

This paper is structured as follows. In Sect. II we give expressions for various differential cross sections relevant to the THM. A detailed critical analysis of the THM experiment is presented in Sect. III. Renormalization procedure for the THM astrophysical factors is described in Sect. IV. Section V presents the renormalized $^{12}C + ^{12}C$ fusion S^* factors obtained by renormalizing the THM astrophysical factors reported in Ref. [1]. Finally, in Sect. VI we highlight the main findings and draw conclusions.

* akram@comp.tamu.edu
† dypang@buaa.edu.cn
‡ a.kadyrov@curtin.edu.au

II. THM DIFFERENTIAL CROSS SECTIONS

A. Triple differential cross section

Let us consider the THM reaction

$$a + A \to s + F^* \to s + b + B, \tag{1}$$

where $a = (s\,x)$ is the Trojan Horse particle and F^* is the resonance in the subsystem $F = (xA)$. The idea of the THM is to extract the information about the binary resonant subreaction

$$x + A \to b + B. \tag{2}$$

The TH reaction is a two-step reaction proceeding through the intermediate resonance. The first step is the transfer reaction $a + A \to s + F^*$ populating the resonance state F^*, which on the second stage decays into the two-body channel $b + B$. Here we present equations which will be used in the following sections. The energy conservation in the center-off-mass (c.m.) of the TH reaction reads

$$E_{aA} - \varepsilon_{sx} = E_{sF} + E_{xA} = E_{sF} + E_{bB} - Q_{if}, \tag{3}$$

where $E_{\alpha\beta} = k^2_{\alpha\beta}/(2\,\mu_{\alpha\beta})$, $Q_{if} = m_x + m_A - m_b - m_B$, $E_{\alpha\beta}$, $\mathbf{k}_{\alpha\beta}$ and $\mu_{\alpha\beta}$ are the relative energy, relative momentum and reduced mass of the particles α and β, m_α is the mass of the particle α, ε_{sx} is the binding energy of the particles s and x in the TH particle $a = (sx)$.

We introduce now a resonance energy in the subsystem $x + A$: $E_{R(xA)} = E_{0(xA)} - i\,\Gamma/2$, $E_{0(xA)}$ is the real part of the resonance energy in the channel $x + A$, Γ is the total resonance width of the resonance F^* populated in the transfer reaction. We consider a two-state coupled channel problem in which the resonance formed in the channel $i = x + A$ decays into a different channel $f = b + B$. Therefore, when in the channel i $E_{xA} \to E_{R(xA)}$ the relative energy E_{bB} approaches the resonance energy $E_{R(bB)}$ in the channel f: $E_{R(bB)} = E_{0(bB)} - i\,\Gamma/2$. For $E_{xA} \to E_{R(xA)}$, due to energy conservation [see (3)], one gets that $E_{sF} \to E_R$, where

$$E_R = E_0 - i\,\Gamma/2. \tag{4}$$

Here

$$E_0 = E_{aA} - \varepsilon_{sx} - E_{0(xA)} = E_{aA} - \varepsilon_{sx} + Q_{if} - E_{0(bB)} \tag{5}$$

is the real part of the resonance energy in the system $s + F$.

The triple DCS at $k_{bB} \to k_{0(bB)}$ is given by [9]

$$\frac{d^3\sigma}{d\Omega_{k_{bB}} d\Omega_{k_{sF}} dE_{sF}} = \frac{\mu_{aA}\mu_{sF}}{(2\pi)^3}\frac{k_0}{k_{aA}}\frac{k_{0(bB)}}{\mu_{bB}}\overline{\left|\mathcal{M}_R\right|^2}, \tag{6}$$

where

$$\begin{aligned}
\overline{\left|\mathcal{M}_R\right|^2} =& \frac{1}{\hat{J}_a\hat{J}_A}\sum_{M_B M_b M_s M_a M_A}\left|M_{M_B M_b M_s;M_A M_a}(k_0\hat{\mathbf{k}}_{sF},\mathbf{k}_{bB},\mathbf{k}_{aA})\right|^2 \\
=& \frac{1}{\hat{J}_a\hat{J}_A}\sum_{M_F M'_F M_A M_a M_s} M_{M_F M_s;M_A M_a}(k_0\hat{\mathbf{k}}_{sF},\mathbf{k}_{aA})\left[M_{M'_F M_s;M_A M_a}(k_0\hat{\mathbf{k}}_{sF},\mathbf{k}_{aA})\right]^* \\
&\times\frac{|N_C|^2}{(E_0 - E_{sF})^2 + \Gamma^2/4}\sum_{M_B M_b} W^{M_F}_{M_B M_b}(\mathbf{k}_{0(bB)})\left[W^{M'_F}_{M_B M_b}(\mathbf{k}_{0(bB)})\right]^*,
\end{aligned} \tag{7}$$

$M_{tr} = M_{M_F M_s;M_A M_a}(k_R\hat{\mathbf{k}}_{sF},\mathbf{k}_{aA})$ is the $a + A \to s + F^*$ transfer reaction amplitude and

$$\begin{aligned}
W^{M_F}_{M_B M_b}(k_{0(bB)}) =& \sqrt{4\,\pi}\sum_{l_b j_b m_{l_b}\nu_b}\left\langle j_b\nu_b\, J_B M_B\middle| J_F M_F\right\rangle \\
&\times\left\langle l_b m_{l_b}\;\, J_b M_b\middle| j_b\nu_b\right\rangle Y_{l_b m_{l_b}}(\mathbf{k}_{0(bB)}) \\
&\times e^{i\,\delta^p(k_{0(bB)})}\sqrt{\frac{\mu_{bB}\,\Gamma_{(bB)}}{k_{0(bB)}}}
\end{aligned} \tag{8}$$

is the vertex form factor for the resonance decay $F^* \to b + B$. Here, J_i (M_i) is the spin (its projection) of particle i, $\hat{J} = 2J + 1$, l_b (m_{l_b}) is the $b - B$ relative orbital angular momentum (its projection) in the resonance F^*, j_b (ν_b) is the total angular momentum (its projection) of particle b in the resonance and $\delta^p(k_{0(bB)})$ is the potential scattering phase shift in the bB channel. Taking into account that

$$\left|\Gamma[1 + i\,\eta]\right|^2 = \frac{\pi\,\eta}{\sinh(\pi\,\eta)} \tag{9}$$

we get the Coulomb renormalization factor N_C [10]

$$|N_C|^2 = \frac{\sinh[\pi(\eta_{sb}+\eta_{sB})]}{\sinh(\pi\eta_{sb})\sinh(\pi\eta_{sB})}\,\frac{\pi\eta_{sb}\eta_{sB}}{(\eta_{sb}+\eta_{sB})}\,\frac{\pi\eta_{\zeta}}{\sinh(\pi\eta_{\zeta})} \times |F(-i\eta_{sB},-i\eta_{sb},1;-1)|^2 \times \exp\left[2\zeta\arctan\frac{2(E_{0(bB)}-E_{bB})}{\Gamma}\right], \quad (10)$$

where

$$\zeta = \eta_{bs}+\eta_{Bs}-\eta_R, \quad (11)$$

$\eta_{ij} = (Z_i\,Z_j/137)\,\mu_{ij}/k_{ij}$, $\eta_R = Z_s\,Z_F\,\mu_{sF}/k_R$, Z_i is the charge of particle i.

It is convenient to integrate the triple DCS over $\Omega_{\mathbf{k}_{bB}}$ to get the double DCS [9], which is expressed in terms of the DCS of the reaction $a+A\to s+F^*$ corresponding to the first step of the TH reaction. However, in the case under consideration, due to the presence of the Coulomb renormalization factor N_C, the DCS obtained from integrating the triple DCS over $\Omega_{\mathbf{k}_{bB}}$ cannot be expressed in terms of the DCS of the first step. The reason is that N_C depends on the integration variable $\Omega_{\mathbf{k}_{bB}}$. However, in the following cases one can neglect this dependence:

1. When $|\eta_{sb}| \ll 1$ and $\eta_{sB} \approx \eta_0$, where $\eta_0 = Z_s\,Z_F\,\mu_{sF}/k_0$, the imaginary part of η_R can be neglected because of the narrow resonance. In this case, $|N_C| \approx 1$ and the integration over $\Omega_{\mathbf{k}_{sF}}$ can be performed without any complications.

2. When $|\eta_{sb}| \ll 1$ and $m_B \gg m_s, m_b$. Let us choose as independent variables the Galilean momenta $\mathbf{k}_s = \mathbf{k}_{sF}$ and $\mathbf{k}_{bB}$. Then one can write

$$\mathbf{k}_{sB} = \frac{m_B\,M}{m_{sB}\,m_{bB}}\,\mathbf{k}_{sF} + \frac{m_s}{m_{sB}}\,\mathbf{k}_{bB} \approx \mathbf{k}_{sF}. \quad (12)$$

Then $\eta_{sB} = (Z_s\,Z_B/137)\,\mu_{sB}/k_{sF}$ and N_C does not depend on $\mathbf{k}_{bB}$ and integration over $\Omega_{\mathbf{k}_{bB}}$ can be performed in a straightforward way.

For the TH reaction under consideration both cases can be applied. We assume that $|N_C| = 1$. Then we can integrate the triple DCS over $\Omega_{\mathbf{k}_{bB}}$ using orthogonality of the spherical harmonics to get the double DCS:

$$\frac{d\sigma}{d\Omega_{\mathbf{k}_{sF}}dE_{sF}} = \frac{1}{2\,\pi}\,\frac{\Gamma_{bB}}{(E_{0(bB)}-E_{bB})^2+\Gamma^2/4}\,\frac{d\sigma}{d\Omega_{\mathbf{k}_{sF}}}, \quad (13)$$

where

$$\frac{d\sigma}{d\Omega_{\mathbf{k}_{sF}}} = \frac{\mu_{aA}\mu_{sF}}{4\pi^2}\,\frac{k_{sF}}{k_{aA}} \sum_{M_F M_s M_A M_a} \times |M_{M_F M_s;M_A M_a}(k_0\hat{\mathbf{k}}_{sF},\mathbf{k}_{aA})|^2 \quad (14)$$

is the DCS of the reaction $a+A\to s+F^*$. Note that integrating over E_{sF} gives

$$\int_0^{\infty} dE_{sF}\frac{d\sigma}{d\Omega_{\mathbf{k}_{sF}}dE_{sF}} = \frac{\Gamma_{bB}}{\Gamma}\,\frac{d\sigma}{d\Omega_{\mathbf{k}_{sF}}}, \quad (15)$$

where Γ_{bB} is the partial resonance width for the decay of the resonance to the channel $b+B$.

B. Double differential cross section of THM reactions proceeding though resonance in the binary subsystem in the intermediate state

In the THM it is enough to consider the double DCS $d\sigma/(d\Omega_{\mathbf{k}_{sF}}dE_{sF})$ from which one needs to single out the astrophysical $S(E_{xA})$ factor for the two-coupled channel resonant binary subreaction

$$x+A\to F^*\to b+B \quad (16)$$

at $E_{xA}\to E_{R(xA)}$, where $E_{R(xA)} = E - i\,\Gamma/2$ is the resonance energy in the channel $x+A$,

$$S(E_{xA}) \overset{E_{xA}\to E_{R(xA)}}{=} \frac{\hat{J}_F}{\hat{J}_x\,\hat{J}_A}\,\frac{5\,\pi}{\mu_{xA}}\,\lambda_N^2\,m_u\,e^{2\,\pi\,\eta_{xA}} \times \frac{\Gamma_{bB}\,\Gamma_{xA}}{\left(E_{R(xA)}-E_{xA}\right)^2+\Gamma^2/4}, \quad (17)$$

$m_u = 931.5$ MeV is the atomic mass unit. Comparing Eqs. (17) and (13) one can observe that to single out the $S(E_{xA})$ astrophysical factor from the latter it is enough to single out from the DCS $d\sigma/d\Omega_{k_{sF}}$ the resonance width Γ_{xA}. To this end in what follows we consider the transformation of the Coulomb DWBA reaction amplitude $M_{M_F M_s;M_A M_a}(k_0\hat{\mathbf{k}}_{sF},\mathbf{k}_{aA})$ describing the transfer reaction $a+A\to s+F^*$ populating the resonance state F^*. This amplitude represents the first step of the THM reaction. The Coulomb DWBA means that the distorted waves in the initial and final states and the optical potentials in the transition operator are the Coulomb ones. The reason for using the Coulomb approximation is based on the fact that in THM only the energy dependence of the DCS is measured. The inclusion of the nuclear interactions do not change significantly this energy dependence, which can be very reasonably approximated by the PWA. However, the Coulomb interactions can significantly affect the energy dependence of the THM DCS when energies are near or below the Coulomb barrier.

The Coulomb DWBA transfer reaction amplitude in the prior form is given by

$$M_{M_F M_s;M_A M_a}(k_0\hat{\mathbf{k}}_{sF},\mathbf{k}_{aA}) = \sum_{m_{s_{xA}} m_{l_{xA}} M_x} \big\langle s_{xA} m_{s_{xA}}\, l_{xA} m_{l_{xA}} \big| J_F M_F \big\rangle \big\langle J_x M_x\ J_A M_A \big| s_{xA} m_{s_{xA}} \big\rangle \times \big\langle s_{sx} m_{s_{sx}}\, l_{sx} m_{l_{sx}}\ \big|\ J_a M_a \big\rangle \big\langle J_s M_s\ J_x M_x \big| s_{sx} m_{s_{sx}} \big\rangle L^{DW(prior)}, \tag{18}$$

with

$$L^{DW(prior)} = \big\langle \Psi^{C(-)}_{\mathbf{k}_{sF}}\, \tilde{\phi}_{R(xA)} \big| V_{sA} + V_{xA} - U^C_{aA} \big| \phi_{sx}\, \Psi^{C(+)}_{\mathbf{k}_{aA}} \big\rangle. \tag{19}$$

Here s_{ij} ($m_{s_{ij}}$) is the channel spin (its projection) in the channel $i+j$, l_{ij} ($m_{l_{ij}}$) is the relative orbital angular momentum of particles i and j, J_i (M_i) is the spin (its projection) of particle i.

We use a three-body model of three constituents s, x and A, all assumed to be structureless particles. In a more general approach we need to introduce the projection operators to ensure that particles x and A are in the ground states in the intermediate states of the transfer reaction. In this case the bound-state wave function ϕ_{sx} and the resonance wave function $\phi_{R(xA)}$ given by Eq. (36) of Ref. [10], should be replaced by the overlap functions. These overlap functions can be approximated by the product of the two-body wave functions and the square roots of the corresponding spectroscopic factors. Because in the THM only the energy dependence of the DCS are measured, these spectroscopic factors can be dropped. In addition, here we use the two-body wave functions rather than the overlap functions.

The matrix element in Eq. (19) involves integration over variable r_{xA}. Following Ref. [2] we can split the integral into the internal part, $r_{xA} < R_{ch}$ and the external part, $r_{xA} \geq R_{ch}$:

$$L^{DW(prior)} = L^{DW(prior)}_{int} + L^{DW(prior)}_{ext}, \tag{20}$$

where

$$L^{DW(prior)}_{int} = \big\langle \Psi^{C(-)}_{\mathbf{k}_{sF}}\, \tilde{\phi}_{R(xA)} \big| V_{sA} + V_{xA} - U^C_{dA} \big| \phi_{sx}\, \Psi^{C(+)}_{\mathbf{k}_{aA}} \big\rangle \Big|_{r_{xA}<R_{ch}} \tag{21}$$

and

$$L^{DW(prior)}_{ext} = \big\langle \Psi^{C(-)}_{\mathbf{k}_{sF}}\, \tilde{\phi}_{R(xA)} \big| V_{sA} + V_{xA} - U^C_{dA} \big| \phi_{sx}\, \Psi^{C(+)}_{\mathbf{k}_{aA}} \big\rangle \Big|_{r_{xA}\geq R_{ch}}. \tag{22}$$

Here, R_{ch} is the channel radius, which is chosen so that at $r_{xA} > R_{ch}$ the nuclear $x-A$ interaction can be neglected.

It was shown in Ref. [2] that

$$L^{DW(prior)}_{int} = L^{DW(post)}_{int} + L^{DW(prior)}_{S}, \tag{23}$$

where

$$L^{DW(post)}_{int} = \big\langle \Psi^{C(-)}_{\mathbf{k}_{sF}}\, \tilde{\phi}_{R(xA)} \big| V_{sx} + V_{sA} - U^C_{sF} \big| \phi_{sx}\, \Psi^{C(+)}_{\mathbf{k}_{aA}} \big\rangle \Big|_{r_{xA}<R_{ch}}, \tag{24}$$

and

$$\begin{aligned} L^{DW(prior)}_{S} =& \big\langle \Psi^{C(-)}_{\mathbf{k}_{sF}}\, \tilde{\phi}_{R(xA)} \big| \overleftarrow{T}_{xA} - \overrightarrow{T}_{xA} \big| \phi_{sx}\, \Psi^{C(+)}_{\mathbf{k}_{aA}} \big\rangle \Big|_{r_{xA}=R_{ch}} \\ =& \frac{R^2_{ch}}{2\mu_{xA}} \int d\mathbf{r}_{sF} \Psi^{C(+)}_{-\mathbf{k}_{sF}}(\mathbf{r}_{sF}) \int d\Omega_{\mathbf{r}_{xA}} \\ & \times \Big[\phi_{sx}(\mathbf{r}_{sx})\, \Psi^{C(+)}_{\mathbf{k_{aA}}}(\mathbf{r}_{aA}) \frac{\partial \phi_{R(xA)}(\mathbf{r}_{xA})}{\partial r_{xA}} - \phi_{R(xA)}(\mathbf{r}_{xA}) \frac{\partial \phi_{sx}(\mathbf{r}_{sx}) \Psi^{C(+)}_{\mathbf{k_{aA}}}(\mathbf{r}_{aA})}{\partial r_{xA}} \Big] \Big|_{r_{xA}=R_{ch}}, \end{aligned} \tag{25}$$

where T_{xA} is the kinetic energy operator of the relative motion of particles x and A. An arrow above the operator points to the direction of its action.

Let us consider now the external matrix element corresponding to $r_{xA} > R_{ch}$. In the external region $V_{sA} + V_{xA} - U^C_{aA} \approx V^C_{sA} + V^C_{xA} - U^C_{sF}$. The distance between s and x is limited because of the presence of the bound-state wave function ϕ_{sx}. Because s and x are close to each other the external matrix element containing the transition operator $V^C_{sA} + V^C_{xA} - U^C_{sF}$ should be small.

The internal matrix element consists of two terms, the internal post-form Coulomb DWBA amplitude $L^{DW(post)}_{int}$ and the surface term $L^{DW(prior)}_{S}$. The internal Coulomb or Coulomb+nuclear DWBA in the post form

should be small due to the highly oscillatory behavior of the binned resonance wave functions (this will be demonstrated in the next section). Note also that the smaller the resonance energy the smaller is the contribution of the internal region.

Then the dominant contribution to the matrix element $L^{DW(prior)}$ comes from the surface term $L_S^{DW(prior)}$. We transform now the surface matrix element into zero-range DWBA amplitude. To this end we use

$$\mathbf{r}_{aA} = \mathbf{r}_{xA} + \frac{m_s}{m_{sx}}\,\mathbf{r}_{sx}, \qquad \mathbf{r}_{sF} = \frac{m_A}{m_{xA}}\,\mathbf{r}_{xA} + \mathbf{r}_{sx}. \quad (26)$$

Rewriting the wave functions $\Psi^{C(+)}_{\mathbf{k}_{aA}}(\mathbf{r_{aA}})$ and $\Psi^{C(+)}_{-\mathbf{k}_{sF}}(\mathbf{r}_{sF})$ in the momentum space we get

$$L_S^{DW(prior)} = \frac{R_{ch}^2}{2\mu_{xA}} \int d\mathbf{r}_{sF} \int \frac{\mathrm{d}\mathbf{p}_{sF}}{(2\,\pi)^3} \int \frac{\mathrm{d}\mathbf{p}_{aA}}{(2\,\pi)^3}\, \Psi^{C(+)}_{\mathbf{k}_{sF}}(\mathbf{p}_{sF})\, \Psi^{C(+)}_{\mathbf{k}_{aA}}(\mathbf{p_{aA}})\, \phi_{sx}(\mathbf{r}_{sx}) e^{-i\mathbf{p}_{sx}\cdot\mathbf{r}_{sx}} \int d\Omega_{\mathbf{r}_{xA}}$$
$$\times \left[e^{i\mathbf{p}_{xA}\cdot\mathbf{r}_{xA}}\, \frac{\partial \phi_{R(xA)}(\mathbf{r}_{xA})}{\partial r_{xA}} - \phi_{R(xA)}(\mathbf{r}_{xA})\, \frac{\partial\, e^{i\mathbf{p}_{xA}\cdot\mathbf{r}_{xA}}}{\partial r_{xA}} \right]\Big|_{r_{xA}=R_{ch}}, \quad (27)$$

where

$$\mathbf{p}_{xA} = \mathbf{p}_{aA} - \frac{m_A}{m_F}\mathbf{p}_{sF}, \qquad \mathbf{p}_{sx} = \mathbf{p}_{sF} - \frac{m_s}{m_a}\,\mathbf{p}_{aA}. \quad (28)$$

Taking into account that $r_{xA} = R_{ch}$ is larger than the nuclear interaction radius we replace the relative $\mathbf{p}_{xA}$ by the on-the-energy-shell (ONES) momentum $\mathbf{k}_{(xA)} = \mathbf{k}_{aA} - \frac{m_A}{m_F}\mathbf{k}_{sF}$. We consider $L_S^{DW(prior)}$ at the real part of the (xA) resonance energy , i.e., $k_{xA} = k_{0(xA)}$ and $k_{sF} = k_0$. Then returning to the coordinate-space representation for $L_S^{DW(prior)}$ we get

$$L_S^{DW(prior)} = \frac{R_{ch}^2}{2\mu_{xA}}\, \mathcal{M}^{DWZR(prior)} \int d\Omega_{xA} \left[e^{-i\mathbf{k}_{0(xA)}\cdot\mathbf{r}_{xA}}\, \frac{\partial \phi_{R(xA)}(\mathbf{r}_{xA})}{\partial r_{xA}} - \phi_{R(xA)}(\mathbf{r}_{xA})\, \frac{e^{-i\mathbf{k}_{0(xA)}\cdot\mathbf{r}_{xA}}}{\partial r_{xA}} \right]\Big|_{r_{xA}=R_{ch}}. \quad (29)$$

Here,

$$\mathcal{M}^{DWZR(prior)} = \int d\mathbf{r}_{sx}\, \Psi^{C(+)}_{-\mathbf{k}_0}(\mathbf{r}_{sx})\, \phi_{sx}(\mathbf{r}_{sx}) \Psi^{C(+)}_{\mathbf{k_{aA}}}\left(\frac{m_s}{m_a}\mathbf{r}_{sx}\right). \quad (30)$$

is the DWBA amplitude, which does not depend on the resonant wave function $\phi_{R(xA)}$ and V_{xA} potential. This equation looks like the zero-range DWBA (ZRDWBA). However, in contrast to the standard zero-range approximation, Eq. (30) can be used for arbitrary value of the orbital momentum of the resonance state (xA).

Note that replacing in Eq. (30) the distorted waves by the plane waves leads to the PWA introduced in [5] and used in [1].

Integrating over $\Omega_{\mathbf{r}_{xA}}$ and using Eq. (36) from [10] for the external resonant wave function we arrive at

$$L_S^{DW(prior)} = e^{-i\,\delta^p(k_{0(xA)})} \sqrt{\frac{1}{\mu_{xA}\,k_{0(xA)}}\,\Gamma_{xA}}\,\frac{1}{2}\,O_{l_{xA}}(k_{0(xA)}R_{ch})\,\mathcal{M}^{DWZR(prior)} i^{-l_{xA}}\,Y_{l_{xA},m_{l_{xA}}}(\widehat{\mathbf{k}}_{0(xA)})\mathcal{W}_{l_{xA}}(E,R_{ch}), \quad (31)$$

where

$$\mathcal{W}_{l_{xA}}(E,R_{ch}) = \left[j_{l_{xA}}(k_{0(xA)}r_{xA}) \left[R_{ch}\,\frac{\partial \ln[O_{l_{xA}}(k_{0(xA)}r_{xA})]}{\partial r_{xA}} - 1 \right] - R_{ch}\,\frac{\partial j_{l_{xA}}(k_{0(xA)}r_{xA})}{\partial r_{xA}} \right]\Big|_{r_{xA}=R_{ch}}. \quad (32)$$

Since $L_S^{DW(prior)}$ gives a dominant contribution, we use $L^{DW(prior)} \approx L_S^{DW(prior)}$. Substituting $L_S^{DW(prior)}$ for $L^{DW(prior)}$ in Eq. (18) we get

$$M_{M_F M_s;M_A M_a}(k_0\hat{\mathbf{k}}_{sF},\mathbf{k}_{aA}) = i^{-l_{xA}} e^{-i\,\delta^p(k_{0(xA)})} \sqrt{\frac{1}{\mu_{xA}\,k_{0(xA)}}\,\Gamma_{xA}}\,\frac{1}{2}\,O_{l_{xA}}(k_{0(xA)}R_{ch})\,j_{l_{xA}}(k_{0(xA)}R_{ch})$$
$$\times\, \mathcal{W}_{l_{xA}}\,Y_{l_{xA},m_{l_{xA}}}(\widehat{\mathbf{k}}_{0(xA)})\, M^{DWZR(prior)}_{M_F M_s;M_A M_a}(k_0\hat{\mathbf{k}}_{sF},\mathbf{k}_{aA}), \quad (33)$$

where

$$M^{DWZR(prior)}_{M_F M_s;M_A M_a}(k_0\hat{\mathbf{k}}_{sF},\mathbf{k}_{aA}) = \sum_{m_{s_{xA}} m_{l_{xA}} M_x} \left\langle s_{xA} m_{s_{xA}}\, l_{xA} m_{l_{xA}} \middle| J_F M_F \right\rangle \left\langle J_x M_x\ J_A M_A \middle| s_{xA} m_{s_{xA}} \right\rangle \times \left\langle s_{sx} m_{s_{sx}}\, l_{sx} m_{l_{sx}}\ \middle|\ J_a M_a \right\rangle \left\langle J_s M_s\ J_x M_x \middle| s_{sx} m_{s_{sx}} \right\rangle \mathcal{M}^{DWZR(prior)}. \quad (34)$$

Returning to Eq. (13) we can now rewrite it as

$$\frac{d\sigma^{THM}}{d\Omega_{\mathbf{k}_{sF}} dE_{sF}} = S(E_{xA})\, e^{-2\pi\eta_{xA}}\, P^{-1}_{l_{xA}}(k_{(0)xA}, R_{ch})\, \frac{\hat{J}_x\, \hat{J}_A}{\hat{J}_F}\, \frac{\hat{l}_{xA} R_{ch}}{80\,\pi^2}\, \lambda_N^{-2}\, m_u^{-1}\, \left|\mathcal{W}_{l_{xA}}(E, R_{ch})\right|^2\, \frac{d\sigma^{DWZR(prior)}}{d\Omega_{\mathbf{k}_{sF}}} \quad (35)$$

We assigned to it the superscript "THM" because this double DCS can be used to analyze THM data. We assume that $\widehat{\mathbf{k}}_{0(xA)}$ is directed along the axis z, that is, $Y_{l_{xA},m_{l_{xA}}}\left(\widehat{\mathbf{k}}_{0(xA)}\right) = \sqrt{(2\,l_{xA}+1)/4\,\pi}\,\delta_{m_{l_{xA}}\,0}$. With this for the DCS of the reaction $a + A \to s + F^*$ populating the resonance state F^* we get

$$\frac{d\sigma^{DWZR(prior)}}{d\Omega_{k_{sF}}} = \frac{\mu_{aA}\mu_{sF}}{4\pi^2}\frac{k_{sF}}{k_{aA}} \sum_{M_F M_s M_A M_a} \left|M^{DWZR(prior)}_{M_F M_s;M_A M_a}(k_0\hat{\mathbf{k}}_{sF},\mathbf{k}_{aA})\right|^2. \quad (36)$$

III. CRITICAL ANALYSIS OF THE THM EXPERIMENT

A. Kinematics of the THM reaction

In Ref. [1] the normalization of the THM data to the direct data was done in the energy interval $E = 2.5 - 2.63$ MeV, where E is the $^{12}\mathrm{C} - {}^{12}\mathrm{C}$ relative kinetic energy. Here and in what follows we use $E_{xA} \equiv E$. To check whether the PWA is justified, we consider the kinematics of the THM in the energy interval covered by the THM experiment [1]. In the THM experiment [1] the relative $^{14}\mathrm{N} - {}^{12}\mathrm{C}$ energy in the entrance channel is $E_{aA} = 13.845$ MeV. From energy conservation in the THM reaction, see Eq. (3), it follows that $E_{aA} + Q = E_f$, where $E_f = E_{sF} + E_{bB}$ is the total kinetic energy of the final three-body system $s+b+B$ and $Q = m_a + m_A - m_s - m_b - m_B$. From this equation we get that the total kinetic energy in the final $d + p + {}^{23}\mathrm{Na}$ channel is $E_f = 5.8$ MeV.

Let us consider the $^{12}\mathrm{C} - {}^{12}\mathrm{C}$ relative energy $E = 2.63$ MeV [1] which is the highest point of the THM normalization interval. For the binary reaction $^{12}\mathrm{C} + {}^{12}\mathrm{C} \to p + {}^{23}\mathrm{Na}$, we have $Q_2 = 2.24$ MeV, where $Q_2 = m_x + m_A - m_b - m_B$. Accordingly, the energy in the $p + {}^{23}\mathrm{Na}$ channel corresponding to $E = 2.63$ MeV is $E_{p\,^{23}\mathrm{Na}} = 4.87$ MeV. Hence, the relative kinetic energy of the deuteron and the c.m. of the $p + {}^{23}\mathrm{Na}$ system corresponding to this energy is $E_{d\,^{24}\mathrm{Mg}} = 0.93$ MeV. This energy is well bellow the Coulomb barrier in the $d - {}^{24}\mathrm{Mg}$ system, which is about 3 MeV. Even on the lower end of the normalization interval corresponding to $E = 2.5$ MeV, the relative energy is $E_{d\,^{24}\mathrm{Mg}} = 1.06$ MeV.

At the energy of $E = 1.5$ MeV in the $^{12}\mathrm{C} - {}^{12}\mathrm{C}$ channel, which corresponds to the energy $E_{p\,^{23}\mathrm{Na}} = 3.74$ MeV in the exit channel, the relative energy $E_{d\,^{24}\mathrm{Mg}} = 2.06$ MeV. This is still below the Coulomb barrier. Note that the resonance energies that can be observed in the THM experiment are $E < 3.56$ MeV. This is due to the fact that at $E > 3.56$ MeV, the resonance energy in the $p + {}^{23}\mathrm{Na}$ channel is $3.56 + Q_2 > 5.8$ MeV. In other words, the $d - {}^{24}\mathrm{Mg}$ relative energy is $E_{d\,^{24}\mathrm{Mg}} < 0$. Even for the energy of $E = 0.805$ MeV, which corresponds to $E_{p\,^{23}\mathrm{Na}} = 3.05$ MeV, the $d - {}^{24}\mathrm{Mg}$ relative energy is $E_{d\,^{24}\mathrm{Mg}} = 2.75$ MeV. The latter is close to but still below the Coulomb barrier.

Figure 1 demonstrates the dependence of $E_{d\,^{24}\mathrm{Mg}}$ on the relative $^{12}\mathrm{C} - {}^{12}\mathrm{C}$ energy E. One can see that within

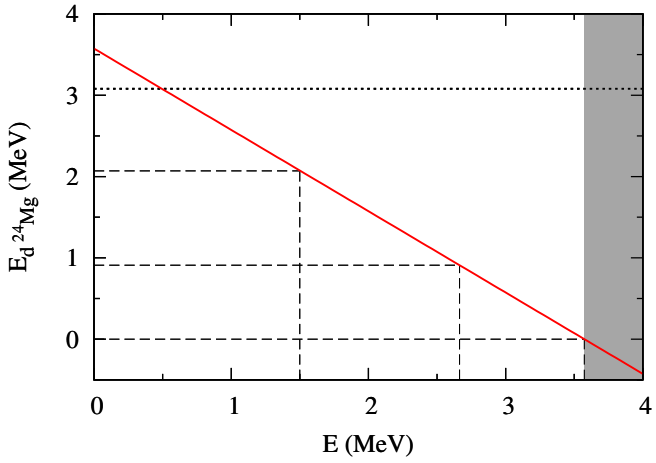

FIG. 1. The dependence of the relative kinetic energy $E_{d\,^{24}\mathrm{Mg}}$ on the relative $^{12}\mathrm{C} - {}^{12}\mathrm{C}$ kinetic energy E. Calculations are done at $E_{^{12}\mathrm{C}\,^{14}\mathrm{N}} = 13.85$ MeV. The grey column is the forbidden area by the energy conservation law. The horizontal dotted line corresponds to the Coulomb barrier in the system $d - {}^{24}\mathrm{Mg}$.

the entire energy interval measured in the THM experiment [1] the energy $E_{d\,^{24}\mathrm{Mg}} < 3$ MeV. Especially low the energy is in the interval $E = 2.5 - 2.63$ MeV used for THM normalization to direct data. Thus we may

conclude that the Coulomb interaction plays a very important role in the energy interval exploited in [1] and, therefore, cannot be neglected.

B. DWBA differential cross section

The presence of the strong Coulomb interaction for such deep sub-Coulomb processes in the final state of the transfer reaction significantly increases the DCS in the backward hemisphere, shifting the peak of the angular distribution of the deuterons to the backward angles. It completely contradicts to the PWA differential cross section in the c.m. system, which has a pronounced peak at forward angles. Even at the lowest observed resonances at $0.8-0.9$ MeV in the THM experiment [1] the angular distribution of the deuterons noticeably deviates from the PWA one if the Coulomb (or Coulomb plus nuclear) rescattering effects in the initial and final states of the ^{12}C transfer reaction are included.

But what is even more important is the fact that the presence of the strong Coulomb interaction significantly changes the absolute values of the DCSs of the ^{12}C transfer reaction and their variation with energy. The absolute values of the DCSs in the THM normalization interval become smaller than the corresponding PWA ones by more than three orders of magnitude and they increase rapidly when the resonance energy decreases. That is one of the main reasons for the drop of the THM astrophysical factors found in this work compared to those extracted in [1] using the PWA.

Below we demonstrate the PWA and DWBA DCSs for the THM reaction. Eq. (35) will be used to obtain the energy dependence of the astrophysical factor. It employs the zero-range DWBAZR DCS. In this DCS the resonance vertex $^{12}\mathrm{C}+{}^{12}\mathrm{C}\rightarrow{}^{24}\mathrm{Mg}^{*}$ is excluded. It allows us to calculate the excitation function in the whole energy interval $E=0.8-2.64$ MeV covered by the THM experiment without need to refer to any specific resonance. This is especially important because some reported resonances in [1] have a negative parity, which is forbidden in collisions of two identical bosons with zero spins. It means that the accuracy of the identification of resonance spins in [1] is ±1. Another important point for using the DWBAZR DCS is related with our intention to renormalize the S factor of the carbon-carbon fusion by taking into account the distortion in the initial and final states. Furthermore, in [1], where a simplified PWA was used, the resonance vertex was completely excluded. The only information about resonance is contained in the factor $\mathcal{W}_{l_{xA}}$, which depends on the orbital angular momentum of the resonance l_{xA}. That is why to be consistent with Ref. [1] we also eliminate the resonance vertex from the DWBA reaction amplitude.

We start by considering the PWA calculations used in [1]. However, in contrast to [1], in our PWA calculations we include the resonance vertex. In each figure we present three different curves corresponding to three different potentials describing the resonance in ^{24}Mg given in Table I. We use the standard notations for the potential parameters shown in Table I: V is the depth of the Woods-Saxon potential, r and a are the radial parameter and the diffuseness.

TABLE I. Parameters of the $^{12}\mathrm{C}-{}^{12}\mathrm{C}$ potentials used to calculate the resonance bin wave functions.

E (MeV)	No.	V (MeV)	r (fm)	a (fm)	width (MeV)
2.7	Potential 1	58.87	1.25	2.40	3.595×10^{-3}
2.7	Potential 2	94.51	1.05	2.40	4.924×10^{-3}
2.7	Potential 3	221.95	1.25	1.85	3.104×10^{-4}
1.5	Potential 1	110.57	2.80	3.05	2.189×10^{-3}
1.5	Potential 2	60.07	2.60	3.05	2.253×10^{-4}
1.5	Potential 3	150.8	2.80	2.30	1.055×10^{-4}
0.8	Potential 1	140.47	4.50	4.50	2.165×10^{-5}
0.8	Potential 2	185.284	4.20	4.50	2.022×10^{-5}
0.8	Potential 3	198.798	4.50	4.04	9.566×10^{-6}

Using the potentials from Table I we make the bin functions for the $^{12}\mathrm{C}-{}^{12}\mathrm{C}$ resonance states. The bins are made by integrating over the $^{12}\mathrm{C}-{}^{12}\mathrm{C}$ scattering wave functions within a range of $^{12}\mathrm{C}-{}^{12}\mathrm{C}$ relative energies centered at the resonant energy with a width of 0.05 MeV. This width corresponds to a typical experimental energy resolution. The bin wave functions are made real by normalization using a factor of $\sin[\delta(k_{^{12}\mathrm{C}\,^{12}\mathrm{C}})]\exp[-i\delta(k_{^{12}\mathrm{C}\,^{12}\mathrm{C}})]$ [11], where $\delta(k_{^{12}\mathrm{C}\,^{12}\mathrm{C}})$ is the $^{12}\mathrm{C}-{}^{12}\mathrm{C}$ scattering phase shift. The bin sizes affect the resulting bin wave functions, and, hence, the amplitude of the THM transfer reaction but they do not affect much the shapes of the angular distributions.

The resonance energies given in Table I are selected from the high end, middle and low energy interval measured in [1]. Note that we are not able to reproduce exactly the location of the resonances reported in [1] but the obtained resonance energy are pretty close to the corresponding experimental ones. The bin wave functions for the three resonance energies constructed using the potentials from Table I are depicted in Fig. 2. The highly oscillatory behavior of the resonance wave functions is a clear evidence that the internal Coulomb or Coulomb+nuclear DWBA in the post form should be small (see Section II B).

The PWA DCSs for three resonance energies $E=2.7$, 1.5 and 0.8 MeV of the $^{12}\mathrm{C}-{}^{12}\mathrm{C}$ system are shown in Fig. 3. Each panel contains three lines corresponding to three different potentials for each resonance energy, see Table I.

Next we show the DWBA DCSs calculated using the bin wave functions shown in Fig. 2. Figure 4 presents the Coulomb DWBA DCSs calculated at the same three resonance energies of the system $^{12}\mathrm{C}-{}^{12}\mathrm{C}$. We performed calculations using the pure Coulomb DWBA (thin lines)

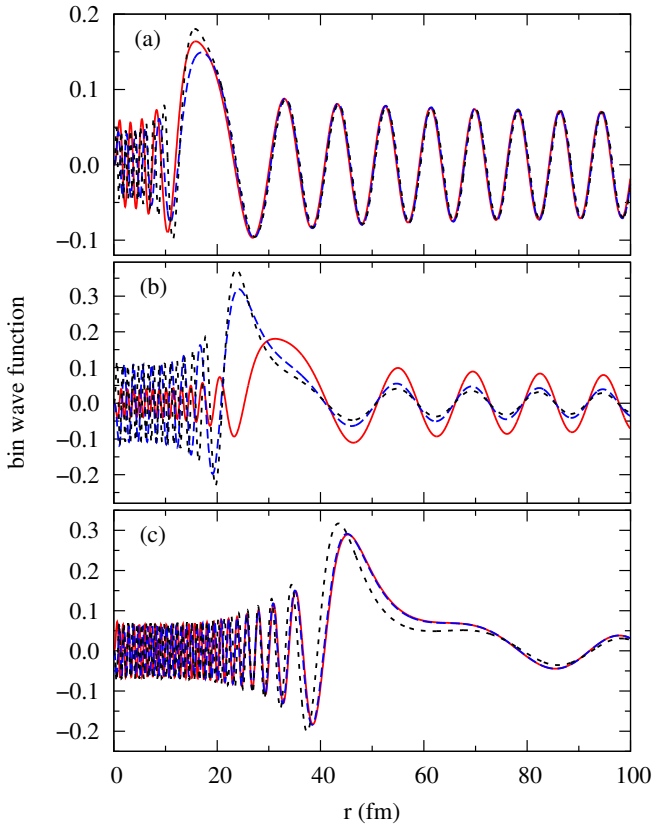

FIG. 2. The bin wave functions calculated for three resonance energies $E = 2.7$, 1.5 and 0.8 MeV of the $^{12}\mathrm{C} - {}^{12}\mathrm{C}$ system. Each panel contains three lines corresponding to three different potentials for each resonance energy. The red solid, blue dashed and black dotted curves correspond to the potentials 1, 2 and 3 from Table I. Panel (a): $E = 2.7$ MeV; panel (b): $E = 1.5$ MeV; panel (c): $E = 0.8$ MeV.

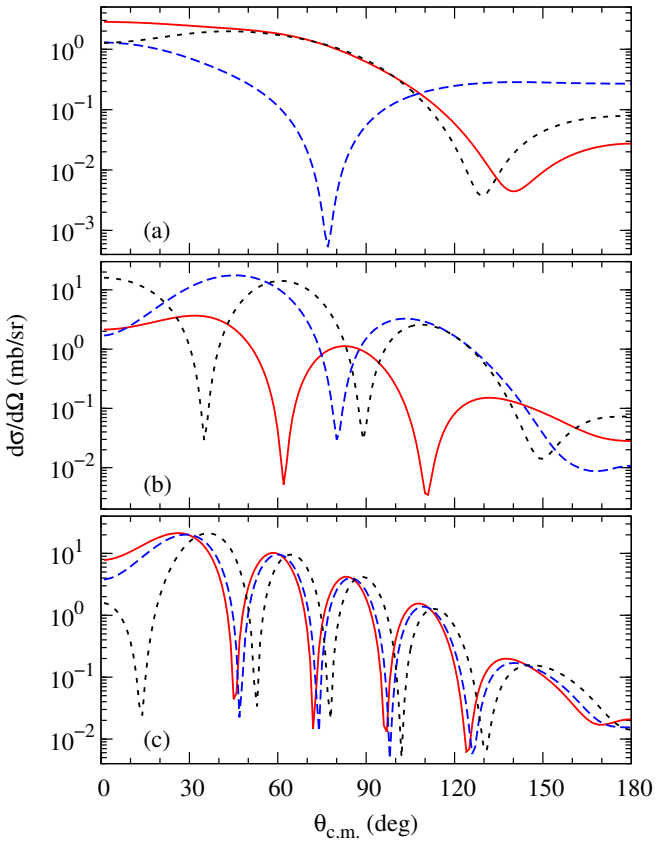

FIG. 3. The PWA DCSs for the $^{14}\mathrm{N} + {}^{12}\mathrm{C} \to d + {}^{24}\mathrm{Mg}^*$ reaction at the relative kinetic energy $E_{^{12}\mathrm{C}\,^{14}\mathrm{N}} = 13.85$ MeV populating three resonant states in ^{24}Mg: $E = 2.7$, 1.5 and 0.8 MeV. Each panel contains three lines corresponding to three different potentials for each resonance energy. The red solid, blue dashed and black dotted curves correspond to the potentials 1, 2 and 3 from Table I. Panel (a): $E = 2.7$ MeV; panel (b): $E = 1.5$ MeV; panel (c): $E = 0.8$ MeV.

and the Coulomb + nuclear DWBA (thick lines). The optical-model potential parameters are taken from the compilation [12], namely, parameters for the $^{14}\mathrm{N} + {}^{12}\mathrm{C}$ potential at 27.3 MeV and the $d + {}^{24}\mathrm{Mg}$ potential at 3.3 MeV are used for the entrance and exit channels, respectively. The relative energy between the deuteron and the c.m. of the ^{24}Mg subsystem depends on the excitation energy of the latter. In principle, different optical potentials should be used in the exit channel for each ^{24}Mg excitation energy. However, our calculations suggest that the DCSs of the transfer reaction depend weakly on the choice of the exit-channel optical model potentials. This is because the relative $d + {}^{24}\mathrm{Mg}$ energies in the exit channel are so low that the Coulomb interaction dominates over the exit-channel distorted waves. For this reason, the same exit-channel optical potential is used for all the cases.

In our approach we use the surface-integral approach, see Ref [2], in which the dominant contribution is given by the external part. To demonstrate that this is indeed the case for the reaction under consideration, in Fig. 5 we present the comparison of the Coulomb DWBA calculated without and with cut-off of the transfer reaction matrix element at $R_{^{12}\mathrm{C}\,^{12}\mathrm{C}} = 7.3$ fm. The latter corresponds to the cut-off radius used in [1] for the PWA calculations.

Finally, we show the deuteron momentum dependence of the Coulomb DWBA DCSs. We introduce the momentum

$$\mathbf{q} = \mathbf{k}_d - \frac{m_d}{m_{^{14}\mathrm{N}}}\,\mathbf{k}_{^{14}\mathrm{N}}, \tag{37}$$

where in the c.m. of the $^{14}\mathrm{N} + {}^{12}\mathrm{C} \to d + {}^{24}\mathrm{Mg}^*$ reaction we have $\mathbf{k}_d = \mathbf{k}_{d\,^{24}\mathrm{Mg}}$ and $\mathbf{k}_{^{14}\mathrm{N}} = \mathbf{k}_{^{14}\mathrm{N}\,^{12}\mathrm{C}}$.

The momentum $\mathbf{q}$ is the Galilean invariant momentum transfer in the $^{14}\mathrm{N} + {}^{12}\mathrm{C} \to d + {}^{24}\mathrm{Mg}^*$ reaction. In the PWA, $\mathbf{q} = \mathbf{q}_{d\,^{12}\mathrm{C}}$ is the $d - {}^{12}\mathrm{C}$ relative momentum. Thus, in the PWA, according to Eq. (37), the $d - {}^{12}\mathrm{C}$ relative momentum is observable because it is expressed in terms of the relative momenta of the particles in the initial and final states of the transfer reaction. At the same time, in the DWBA, due to rescattering of the particles in the initial and final states, it is impossible to determine

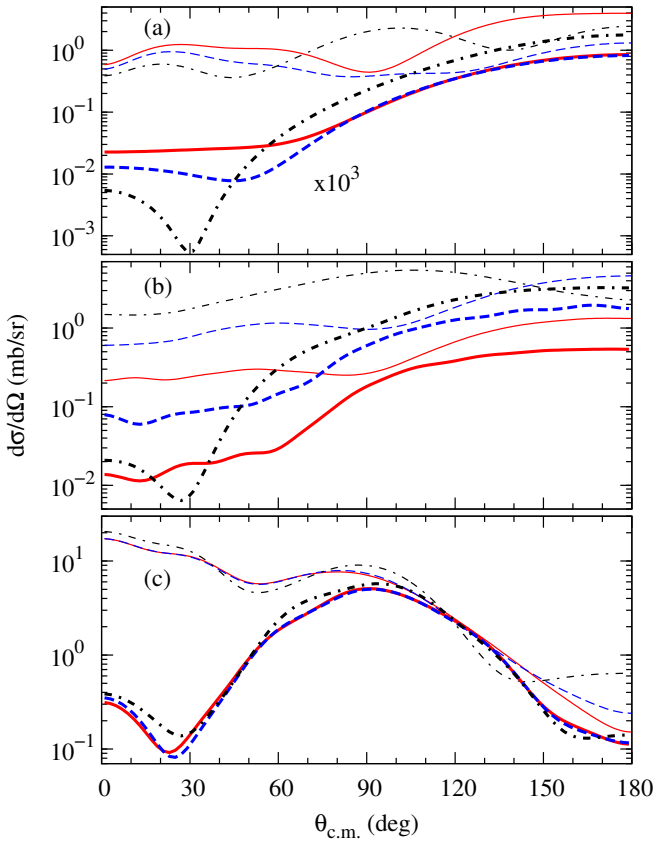

FIG. 4. The DWBA DCSs for the $^{14}\mathrm{N}+{}^{12}\mathrm{C}\to d+{}^{24}\mathrm{Mg}^{*}$ reaction at the relative kinetic energy $E_{^{12}\mathrm{C}\,^{14}\mathrm{N}}=13.85$ MeV populating three resonant states in ^{24}Mg. Panel (a): $E=2.7$ MeV; panel (b): $E=1.5$ MeV and panel (c): $E=0.8$ MeV. Each panel contains six lines. The thin (thick) red solid, blue dashed and black dotted curves correspond to the Coulomb (Coulomb + nuclear) DWBA DCSs calculated using the $^{12}\mathrm{C}-{}^{12}\mathrm{C}$ bin wave functions for the potentials 1, 2 and 3 from Table I, respectively. Note that the DWBA DCSs in panel (a) are multiplied by 10^3.

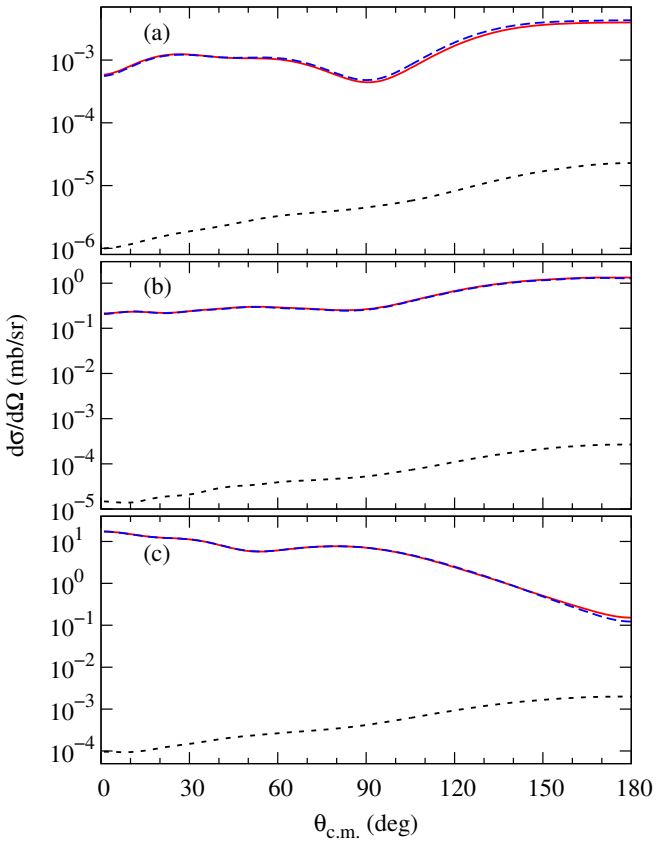

FIG. 5. Comparison of the Coulomb DWBA DCSs for the $^{14}\mathrm{N}+{}^{12}\mathrm{C}\to d+{}^{24}\mathrm{Mg}^{*}$ reaction populating three resonant states in ^{24}Mg calculated with and without cut-off in the matrix element over $r_{^{12}\mathrm{C}\,^{12}\mathrm{C}}$. The solid red lines: the Coulomb DWBA DCSs calculated without cut-off; black dotted line: the internal part of the Coulomb post-form DWBA DCSs calculated for $r_{^{12}\mathrm{C}\,^{12}\mathrm{C}}\le 7.3$ fm; blue dashed line: the external part of the Coulomb post-form DWBA DCSs calculated for $r_{^{12}\mathrm{C}\,^{12}\mathrm{C}}\ge 7.3$ fm. Panel (a): $E=2.7$ MeV; panel (b): $E=1.5$ MeV and panel (c): $E=0.8$ MeV. All the calculations were performed using the bin wave functions for the potential 1 from Table I.

the $d-{}^{12}\mathrm{C}$ relative momentum. Expressing the deuteron scattering angle in terms of $\mathbf{q}$ at fixed k_d and $k_{^{14}\mathrm{N}}$ one can determine the dependence of the DWBA DCS on $\mathbf{q}$. Since $\mathbf{q}=\mathbf{q}_{d\,^{12}\mathrm{C}}$, the dependence of the PWA DCS on q is determined by the momentum dependence of the Fourier transform of the square of the s-wave $d-{}^{12}\mathrm{C}$ bound-state wave function $\phi^2_{d\,^{12}\mathrm{C}}(q)$. By comparing the dependence of the DWBA DCS and $\phi^2_{d^{12}\mathrm{C}}$ on q we can determine the effect of the distortions for the THM reaction and the validity of the PWA.

Using Eq. (37) we get

$$\frac{d\sigma}{dq}=\frac{m_{^{14}N}}{m_d}\frac{q}{k_{d^{24}Mg}k_{^{14}N^{12}C}}\frac{1}{\sin\theta}\frac{d\sigma}{d\theta}, \qquad (38)$$

where $\cos\theta=\hat{\mathbf{k}}_d\cdot\hat{\mathbf{k}}_{^{14}\mathrm{N}}$, $\hat{\mathbf{k}}=\mathbf{k}/k$. The DCS $d\sigma/dq$ calculated for three different resonance energies $E=2.7$, 1.5 and 0.8 MeV and three potentials from Table I are shown in Fig. 6.

From the presented figures we can draw the following conclusions:

- The PWA and the DWBA DCSs differ significantly both in the angular distributions and energy dependences. In particular, the DWBA calculations show that in the interval of the resonance energies $E=1.5-2.7$ MeV the angular distributions have backward peaks in contrast to the PWA ones. This is a very important point. As we will see below, the different energy dependences of the PWA and DWBA DCSs lead to very different energy dependences of the astrophysical factors calculated using the PWA and DWBA.
- The ratio of the DCSs from the PWA and the DWBA at $E=2.7$ MeV and 0.8 MeV are completely different. The DWBA DCSs at any angle at

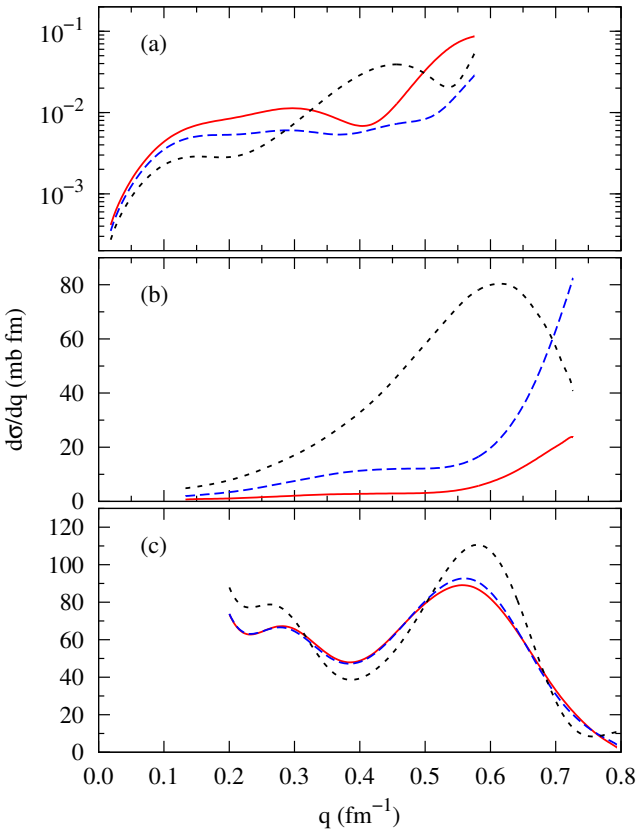

FIG. 6. The Coulomb DWBA DCSs $d\sigma/dq$ for the ^{14}N + ^{12}C $\rightarrow$ d + ^{24}Mg* reaction at the relative kinetic energy $E_{^{12}\mathrm{C}\,^{14}\mathrm{N}}$ = 13.85 MeV populating three resonant states in ^{24}Mg: E = 2.7, 1.5 and 0.8 MeV. Panel (a): E = 2.7 MeV; panel (b): E = 1.5 MeV and panel (c): E = 0.8 MeV. Each panel contains three lines corresponding to three different potentials for each resonance energy. The red solid, blue dashed and black dotted curves correspond to the potentials 1, 2 and 3 from Table I, respectively.

E = 2.7 MeV are significantly smaller than those at E = 0.8 MeV. This happens only if the Coulomb or the Coulomb plus nuclear distortions are taken into account. This is an additional corroboration of the fact that at the resonance energies of the THM normalization interval E = 2.5-2.63 MeV considered in [1], the THM reactions are deep sub-Coulomb. This makes their DWBA DCSs extremely small. The absolute value of the DWBA DCS increases when E decreases because the energy of the outgoing deuteron increases approaching the Coulomb barrier.

As we will see later [see Eq. (41) below] for the S factor the DWBA DCS appears in the denominator. A very small DCS at high E should significantly increase the THM astrophysical factor. As the energy E decreases the DWBA DCS increases and the $S(E)$ factor quickly drops. For comparison we set our renormalization factor $R(E)$ [see Eq. (43) below] equal to unity at E = 2.664 MeV, which is on the upper border of the THM normalization interval considered in [1]. The significant rise of the DWBA DCS toward small E is the factor that most contributes to the drop of the THM $S(E)$.

- The momentum distributions of the deuterons at E = 2.7 and 1.5 MeV completely contradict the momentum distribution of the deuterons given by the Fourier transform of the deuteron bound-state wave function in ^{14}N, see the extended data given in Fig. 1 of Ref. [1]. This serves an additional confirmation that the PWA-based Eq. (2) of Ref. [1] leading to the factorization of the deuteron bound-state wave function is not valid. Note that the resonance energy E = 1.5 MeV corresponds to the most effective astrophysical energy for carbon-carbon fusion.

IV. RENORMALIZATION OF THM ASTROPHYSICAL FACTORS

Thus we have provided a compelling evidence that the Coulomb effects must be included. Next we describe the correct procedure, which shows how the S factors deduced in Ref. [1] should be renormalized taking into account the distortion effects in the initial and final states of the transfer reaction.

We start from the THM double DWBA DCS given by Eq. (35) which can be rewritten as

$$\frac{\mathrm{d}^2\sigma^{\mathrm{THM}}}{\mathrm{d}E\mathrm{d}\Omega_{\mathbf{k}_{sF}}} = K(E)\,S(E)\,\left|\mathcal{W}_{l_{xA}}(E,R_{ch})\right|^2\,\frac{d\sigma^{DWZR(prior)}}{d\Omega_{\mathbf{k}_{sF}}}. \tag{39}$$

Here,

$$K(E) = e^{-2\,\pi\,\eta_{xA}}\,P^{-1}_{l_{xA}}(k_{(0)aA},R_{ch})\,\frac{\hat{J}_x\,\hat{J}_A}{\hat{J}_F}\,\frac{\hat{l}_{xA}R_{ch}}{80\,\pi^2}\,\lambda_N^{-2}\,m_u^{-1} \tag{40}$$

is a trivial kinematical factor, $E \equiv E_{xA}$, $d\sigma^{DWZR(prior)}/d\Omega_{\mathbf{k}_{sF}}$ is the zero-range DWBA cross section of the ^{14}N+^{12}C $\rightarrow$ d+^{24}Mg* reaction populating the isolated resonance state, θ_s is the scattering angle of the spectator s in the c.m. of the THM reaction, $S(E)$ is the astrophysical factor.

Correspondingly, the THM astrophysical factor determined from Eq. (39) is

$$S(E) = \frac{N_F}{K(E)}\,\frac{\mathrm{d}^2\sigma^{\mathrm{THM}}}{\mathrm{d}E\,\mathrm{d}\Omega_{\mathbf{k}_{sF}}}\,\frac{1}{\left|\mathcal{W}_{l_{xA}}(E,R_{ch})\right|^2} \times \frac{1}{\mathrm{d}\sigma^{\mathrm{DWZR(prior)}}(E,\cos\theta_s)/\mathrm{d}\Omega_{\mathbf{k}_{sF}}}. \tag{41}$$

Here N_F is an overall, energy-independent factor for normalization of the THM data to direct data. We recall

that in the THM only the energy dependence of the astrophysical factor is measured. Its absolute value is determined by normalizing the THM $S(E)$ factor to the direct data available at higher energies.

Equations (39) and (41) are pivotal for understanding the problem of extraction of the $S(E)$ factor from the THM differential cross section. Because in the normalization interval of $E = 2.5 - 2.66$ MeV the outgoing deuterons are below the Coulomb barrier, $\mathrm{d}\sigma^{\mathrm{DWZR(prior)}}(E,\cos\theta_s)/\mathrm{d}\Omega_{\mathbf{k}_{sF}}$ is small and rapidly increases when the resonance energy E decreases. This increase of $\mathrm{d}\sigma^{\mathrm{DWZR(prior)}}(E,\cos\theta_s)/\mathrm{d}\Omega_{\mathbf{k}_{sF}}$ should reflect in the behavior of $\mathrm{d}^2\sigma^{\mathrm{THM}}/\mathrm{d}E\,\mathrm{d}\Omega_{\mathbf{k}_{sF}}$ and the THM $S(E)$ factor. As we mentioned, in Ref. [1] a simple PWA was used instead of the distorted waves. The DCS as a function of E_{dF} obtained using the PWA changes very little compared to the change of the DWBA DCS. This is the main reason why the THM $S(E)$ factors show unusually high rise when E decreases.

In [1] the selected normalization interval was chosen to be $E = 2.5 - 2.63$ MeV. However, there are two resonances with negative parities that are questionable because the collision of the two identical bosons $^{12}\mathrm{C} + {}^{12}\mathrm{C}$ cannot populate resonances with the negative parity. There are two resonances with positive parities cited in [1]: at 2.664 and 2.537 MeV. It was underscored in [1] that the THM data reproduce the higher-lying resonance. That is why here we use the resonance at 2.664 MeV for the normalization of the THM data to direct ones. Thus, we assume here that the normalization factor N_F is determined by normalizing the THM astrophysical factor to the directly measured resonance at $E = 2.664$ MeV. Practically we selected the normalization of the THM data on the edge of the energy interval measured in [1].

To find the renormalization of the THM astrophysical factor presented in [1] we recall that in the PWA the THM astrophysical factor for an isolated resonance is given by

$$S^{(\mathrm{PWA})}(E) = \frac{N_F}{K(E)}\,\frac{\mathrm{d}^2\sigma^{\mathrm{THM}}}{\mathrm{d}E\,\mathrm{d}\Omega_{\mathbf{k}_{sF}}}\,\frac{1}{\phi^2_{sx}(E)\,|\mathcal{W}_{l_{xA}}(E,R_{ch})|^2}. \tag{42}$$

The factor $\mathcal{W}_{l_{xA}}$ was obtained in [2], $\phi_{sx}(E)$ is the Fourier transform of the $a = (s\,x)$ bound-state wave function. The Fourier transform, actually, depends on $q = k_{sx}$, which is in the case under consideration is $q = k_{d\,{}^{12}\mathrm{C}}$ and expressed in terms of $\mathbf{k}_d$. From energy conservation, see Eq. (3), it follows that $E_{sF} = E_{aA} - \varepsilon_{sx} - E$, where $E \equiv E_{xA}$ and $E_{sF} = E_s$. Hence the Fourier transform of the bound-state wave function $\phi_{sx}(q)$ depends on E.

By taking the ratio of the $S(E)$ factors given by Eqs. (41) and (42) and normalizing it to unity at $E = E_N$ we get the renormalization factor of the THM astrophysical factor presented in [1], but this time including the Coulomb (Coulomb + nuclear) distorted waves in the initial and final states of the THM transfer reaction

$$R(E) = \frac{\phi^2_{sx}(E)}{\phi^2_{sx}(E_N)}\,\frac{\mathrm{d}\sigma^{\mathrm{DWZR(prior)}}(E_N,\cos\theta_s)/\mathrm{d}\Omega_{\mathbf{k}_{sF}}}{\mathrm{d}\sigma^{\mathrm{DWZR(prior)}}(E,\cos\theta_s)/\mathrm{d}\Omega_{\mathbf{k}_{sF}}}, \tag{43}$$

where E_N is the THM normalization energy.

V. ASTROPHYSICAL FACTORS FOR THE $^{12}\mathrm{C} - {}^{12}\mathrm{C}$ FUSION FROM THM REACTION

In this section we present new $^{12}\mathrm{C} - {}^{12}\mathrm{C}$ fusion S^* factors obtained by renormalizing the THM astrophysical factors presented in [1]. For renormalization the factor $R(E)$ given in Eq. (43) is used. The DWBA DCSs are calculated using the FRESCO code [11]. For comparison we also calculate $\mathrm{d}\sigma^{\mathrm{DWZR(prior)}}(E,\cos\theta_s)/\mathrm{d}\Omega_{\mathbf{k}_{sF}}$ including the nuclear distortions. To calculate the optical-model distorted waves we use the optical potentials from Ref. [12] as described above. Following [1] we use the normalization energy $E_N = 2.664$ MeV.

The Woods-Saxon potential for the bound-state wave function $\phi_{d\,{}^{12}\mathrm{C}}$ has a depth of 34.459 MeV and standard shape: $a = 0.65$ fm and $r_0 = r_C = 1.25$ fm, where r_0 and r_C are the nuclear and the Coulomb radial parameters. With this potential the $^{14}\mathrm{N}$ bound-state wave function has one node away from the origin. The calculated $d-{}^{12}\mathrm{C}$ radial s-wave bound-state wave function and the square of its Fourier transform are shown in Fig. 7. To calculate the Fourier transform of the bound-state wave function as a function of the resonance energy E we use Eq. (37). In the c.m., q^2 depends on $\mathbf{k}_d = \mathbf{k}_{d\,{}^{24}\mathrm{Mg}}$, $\mathbf{k}_{{}^{14}\mathrm{N}} = \mathbf{k}_{{}^{14}\mathrm{N}\,{}^{12}\mathrm{C}}$ and $\cos\theta$, where θ is the deuteron scattering angle in the c.m. of the THM transfer reaction $^{14}\mathrm{N} + {}^{12}\mathrm{C} \to d + {}^{24}\mathrm{Mg}$. We fix the scattering angle at $\theta = 15$ deg and consider $k_{{}^{14}\mathrm{N}}$ fixed taking into account the fact that the experimental $^{14}\mathrm{N} - {}^{12}\mathrm{C}$ relative energy is 13.85 MeV. From Eq. (3), where $E \equiv E_{xA}$, it follows that k_d and, hence, q are functions of E.

To calculate the energy dependence of renormalization factor $R(E)$ we need to know the energy dependence of $|\phi_{d\,{}^{12}\mathrm{C}}(E)|^2$ shown in panel (b) of Fig. 7, and the energy dependence of the DWBAZR DCS, where E is the $^{12}\mathrm{C} - {}^{12}\mathrm{C}$ relative energy at a fixed deuteron scattering angle. As mentioned earlier, employing the DWBAZR DCS where the resonance $^{12}\mathrm{C} - {}^{12}\mathrm{C}$ wave function is excluded, allows us to scan the energy behavior of the DWBA DCS without any information about resonances in the $^{12}\mathrm{C} + {}^{12}\mathrm{C}$ system. The energy dependence of the DWBAZR at the deuteron scattering angle of 15 degree in the c.m. of the reaction is shown in Fig. 8.

The renormalized astrophysical factors are compared with original ones from [1] in Figs. 9 and 10. The renormalized astrophysical factors are $R(E)\,S^*(E)$, where $S^*(E)$ are taken from [1] (here we use the notation for the S factor from [1]). Panel (a) of Fig. 9 shows the behavior of the astrophysical factor for the channel $p_0 + {}^{23}\mathrm{Na}$. As seen in panels (b), (c) and (d), a similar

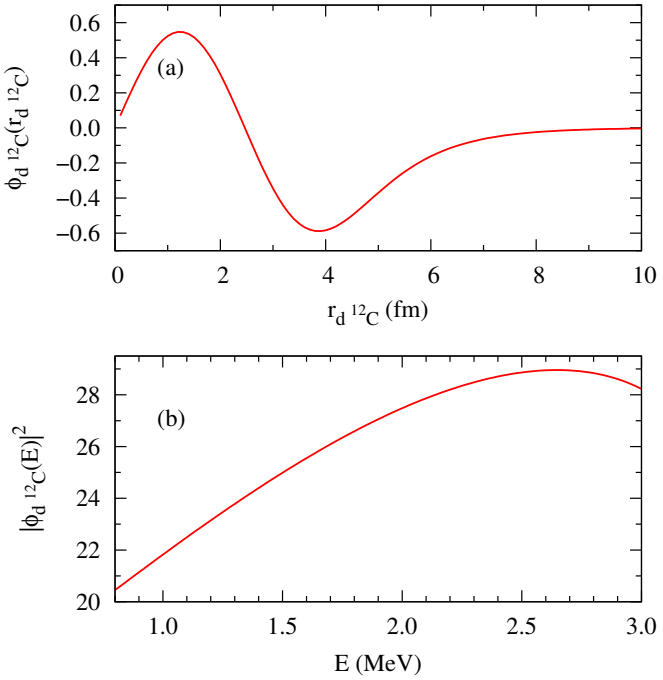

FIG. 7. Panel (a): the $d-^{12}$C radial s-wave bound-state wave function calculated using the Woods-Saxon potential with the depth 34.4588 MeV and the standard parameters, $r_0 = 1.25$ fm and $a = 0.65$ fm. Panel (b): the magnitude-square of the Fourier transform of the $d-^{12}$ C bound-state wave function from panel (a) as a function of the resonance energy E of the $^{12}\mathrm{C} - ^{12}\mathrm{C}$ system.

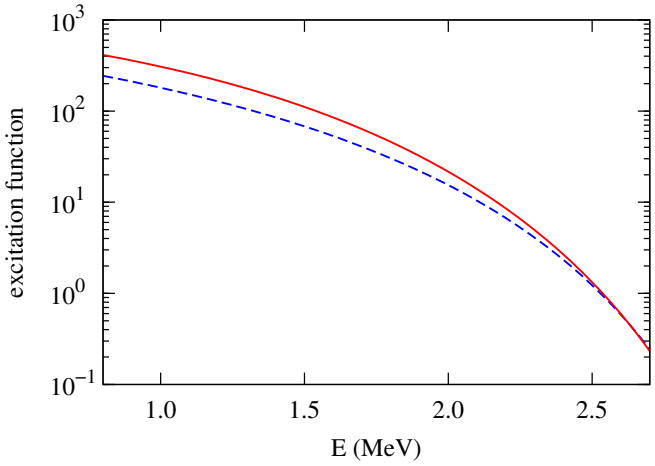

FIG. 8. The excitation function of the THM transfer reaction $^{14}\mathrm{N} + ^{12}\mathrm{C} \to d + ^{24}\mathrm{F}^*$ calculated using the zero-range DWBA at the scattering angle of the deuteron of 15 degree in the c.m. of the reaction. The solid red line is for the pure Coulomb DWBA and the dashed blue line for the Coulomb + nuclear DWBA.

behavior of the $R(E)\,S^*(E)$ factors is found for the three other channels, $p_1 + {}^{23}\mathrm{Na}(0.44\,\mathrm{MeV})$, $\alpha_0 + {}^{20}\mathrm{Ne}$ and $\alpha_1 + {}^{20}\mathrm{Ne}(1.63\,\mathrm{MeV})$. Therefore, in Fig. 10 we show the total astrophysical factors, by summing the astrophysical factors of the four final channels detected in [1]. We find that at the resonance energies $E = 0.8 - 0.9$ MeV the renormalization factor $R(E)$ decreases the THM astrophysical factors from [1] by about a factor of 10^3.

We conclude from Figs. 9 and 10 that the inclusion of the distorted waves in the initial and final states eliminates the sharp raise of the $S^*(E)$ factors extracted in [1] using the THM in the PWA. This constitutes the main result of our paper. In this work we merely renormalized the astrophysical factors reported in [1], taking into account the distorted waves as required. Hence, our renormalized S^* factors do not, and are not supposed to, exhibit new resonances. They just follow the resonance structure of the astrophysical factors obtained in [1].

Our estimations of the DWBA DCSs of the ^{12}C transfer reaction show that in the THM normalization interval of $2.5 - 2.664$ MeV, the DWBA DCSs are of the order of $10^{-4} - 10^{-5}$ mb/sr. Such small DCSs can hardly be measured in the coincidence experiment. That is why the THM data are not reliable at higher energies. The absence in the THM data of a strong isolated resonance at $E \sim 2.1$ MeV observed in Stella experiment [13] confirms the doubts about the quality of the high-energy THM data at $E > 2$ MeV, which is important for normalization of the THM data.

To corroborate our findings further, in Fig. 11 we present the renormalization factors $R(E)$ at three different incident ^{14}N energies: 30, 33 and 35 MeV. The first energy is used in the THM experiment in Ref. [1]. We see a strong drop of $R(E)$ for $E_{^{14}\mathrm{N}} = 30$ MeV . We do not discuss here whether the higher energies would allow one to cover the whole resonance energy interval. We just demonstrate that when the incident energy of ^{14}N increases the renormalization factor quickly approaches unity confirming that the Coulomb distortions are the main reason for the drop of $R(E)$ at 30 MeV. This again confirms that at this energy the simple PWA is not valid.

VI. SUMMARY

The Trojan Horse method is a powerful and unique indirect technique that allows one to measure the astrophysical factors of the resonant reactions at low energies, where direct methods are not able to obtain data due to very small cross sections. A compelling evidence of the power of the THM at astrophysically-relevant energies is clearly demonstrated in [1] by discovering a strong resonance peak in $^{24}\mathrm{Mg}^*$ at $E < 0.9$ MeV. This region is not reachable by any direct method. However, we question the validity of the results for the astrophysical factors reported in [1] using the plane-wave approximation. Since the THM deals with three-body reactions rather than binary ones, a reliable theoretical analysis of the THM data becomes critically important. For the THM reactions with the neutron-spectator or for the reactions with the energies above the Coulomb barrier and for interact-

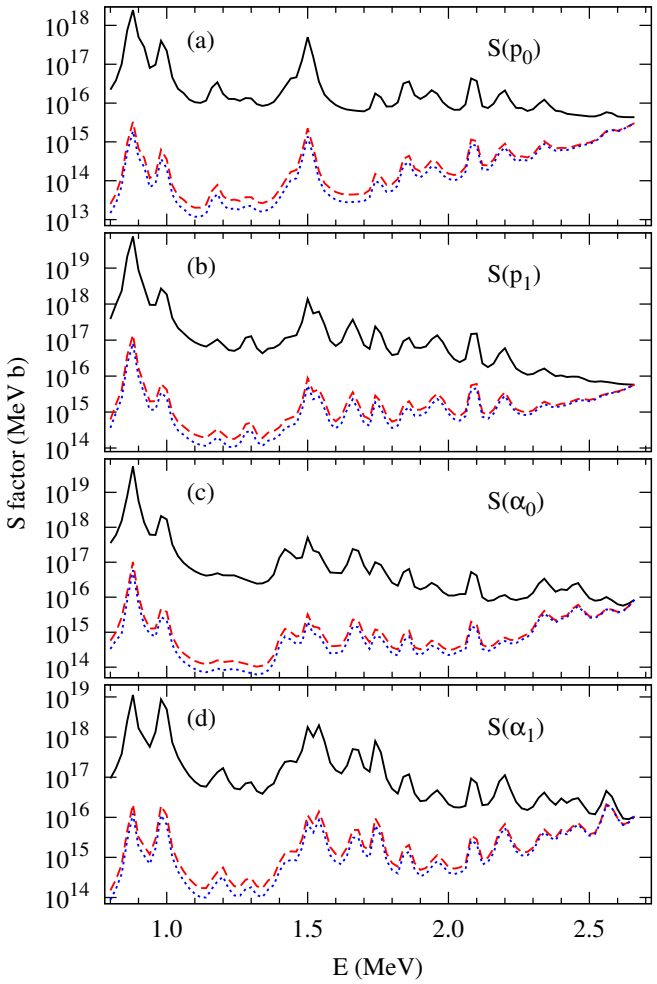

FIG. 9. Astrophysical $S^*(E)$ factors for $^{12}C + ^{12}C$ fusion. Panel (a): $S^*(E)$ factors for the reaction $^{12}C + ^{12}C \to p_0 + ^{23}Na$. Black solid line is the $S^*(E)$ factor from [1]. The red dashed line is the renormalized $R(E)\,S^*(E)$ factor calculated using the pure Coulomb distortions. The blue dotted line is the renormalized $R(E)\,S^*(E)$ factor calculated using the Coulomb plus nuclear distortions. Panel (b): $S^*(E)$ factors for the reaction $^{12}C + ^{12}C \to p_1 + ^{23}Na(0.44\,MeV)$, where the ^{23}Na excitation energy is 0.44 MeV. Panel (c): $S^*(E)$ factors for the reaction $^{12}C + ^{12}C \to \alpha_0 + ^{20}Ne$. Panel (d): $S^*(E)$ factors for the reaction $^{12}C + ^{12}C \to \alpha_1 + ^{20}Ne(1.63\,MeV)$. The notations in panels (b), (c) and (d) are the same as in panel (a).

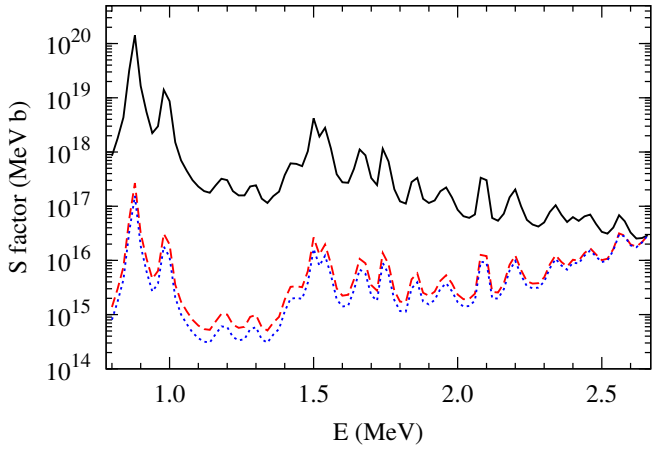

FIG. 10. Total $S^*(E)$ factors for $^{12}C + ^{12}C$ fusion. Black solid line is the $S^*(E)$ factor from [1]. The red dashed line is the renormalized $R(E)\,S^*(E)$ factor calculated using the pure Coulomb distortions. The blue dotted line is the renormalized $R(E)\,S^*(E)$ factor calculated using the Coulomb plus nuclear distortions.

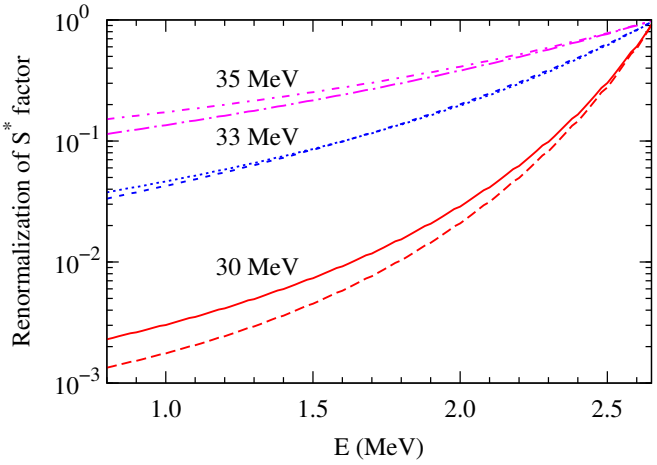

FIG. 11. Renormalization factors $R(E)$ calculated at three different incident energies of ^{14}N. Red lines are $R(E)$ for $E_{^{14}N} = 30$ MeV: solid line is calculated with pure Coulomb distortions, dashed line corresponds to the Coulomb plus nuclear distortions; blue lines are $R(E)$ for $E_{^{14}N} = 33$ MeV: dotted line is for the Coulomb distortions, dash-dotted line is for the Coulomb plus nuclear distortions; magenta lines are $R(E)$ for $E_{^{14}N} = 35$ MeV: dash-dotted-dotted line is for the Coulomb distortions, short dash line is for the Coulomb plus nuclear distortions.

ing nuclei with small charges, the simple PWA works quite well and the THM results are expected to be reliable. However, this is not the case for the THM reaction under consideration, which aims to determine the astrophysical factors of $^{12}C + ^{12}C$ fusion. In this process we deal with the strong Coulomb interactions in the initial and final states of the THM transfer reaction. Moreover, the energies of the deuteron-spectator in the final state are significantly below the Coulomb barrier at the energies of the normalization interval of the THM data to direct ones. We have demonstrated here that the replacement of the PWA by the approach, which takes into account the Coulomb or Coulomb + nuclear distortions, decreases the THM astrophysical factors reported in Ref. [1] at the resonance energies of $E = 0.8 - 0.9$ MeV by up to 10^3 times. We would like to add that the recent most accurate direct measurements, which are extended down to $E = 2.1$ MeV [13] do not agree with the results from [1]. We believe that the problem with the astrophysical factors for the carbon-carbon fusion reaction calls for

new direct and indirect experiments.

VII. ACKNOWLEDGMENTS

A.S.K. acknowledges a support from the Australian Research Council and U.S. NSF Award No. PHY-1415656 during his stay at the Cyclotron Institute, Texas A&M University. A.M.M. acknowledges the support from the U.S. DOE Grant No. DE-FG02-93ER40773, NNSA Grant No. DE-NA0003841 and U.S. NSF Award No. PHY-1415656. D.Y.P. acknowledges the support by the national key research and development program (2016YFA0400502) and the support by NSFC Grant Nos. 11775013 and U1432247.

[1] A. Tumino *et al.*, Nature **557**, 687 (2018).
[2] A. M. Mukhamedzhanov, Phys. Rev. C **84**, 044616 (2011).
[3] A. M. Mukhamedzhanov, D. Y. Pang, C. A. Bertulani, and A. S. Kadyrov, Phys. Rev. C **90** 034604 (2014).
[4] A. S. Kadyrov, I. Bray, A. M. Mukhamedzhanov, and A. T. Stelbovics, Ann. Phys. **324**, 1516 (2009).
[5] R. E. Tribble, C. A. Bertulani, M. La Cognata, A. M. Mukhamedzhanov and C. Spitaleri, Rep. Prog. Phys. **77**, 106901 (2014).
[6] C. Spitaleri, M. La Cognata, L. Lamia, A.M. Mukhamedzhanov , and R. G. Pizzone, Eur. Phys. J. A **52**, 77 (2016).
[7] G. R. Caughlan and W. A. Fowler, Thermonuclear reaction rates V. At. Data Nucl. Data Tables **40**, 283 (1988).
[8] C. Iliadis, Nuclear Physics of Stars (Wiley, Weinheim, 2007).
[9] E. I. Dolinsky, P. O. Dzhamalov and A. M. Mukhamedzhanov, Nucl. Phys. A **202**, 97 (1973).
[10] A. M. Mukhamedzhanov and A. S. Kadyrov, Few-Body Systems **60**, 27 (2019).
[11] I. J. Thompson, Comp. Phys. Rep. **7**, 167 (1988).
[12] C.M. Perey and F.G. Perey, Compilation of phenomenological optical-model parameters 1954-1975, Atom. Data Nucl. Data Tables **17**, 1 (1976).
[13] C. Beck, arXiv: 1812.08013 (2018).